Chronic Neovascular Central Serous Chorioretinopathy: A Stress/Rest Optical Coherence Tomography Angiography Study

MARCO LUPIDI, DANIELA FRUTTINI, CHIARA MARIA EANDI, MASSIMO NICOLÒ, DIOGO CABRAL, SILVIA TITO, CARLO CAGINI, AND FELICE CARDILLO PICCOLINO

• PURPOSE: To compare optical coherence tomography-angiography (OCT-A) performed during physical exercise (stress OCT-A) to the basal examination (rest OCT-A) in the imaging of choroidal neovascularization (CNV) in patients with chronic central serous chorioretinopathy (CSCR).

• DESIGN: Prospective, cohort study.

• METHODS: This multicenter study included 29 consecutive patients with chronic CSCR and flat irregular pigment epithelium detachments (FIPEDs). All patients underwent rest and stress OCT-A (i.e., hand-grip test [HGT]). Systemic hemodynamic data were recorded during the examinations. Rest and stress OCT-A in the en-face and cross-sectional views were qualitatively compared to establish the degree of evidence of flow signals due to CNVs. The en-face angiograms underwent additional automated quantitative analysis to assess the rate of change in neovascular parameters during the stress condition.

• RESULTS: Blood pressure significantly increased during the HGT ($P = 0.001$). Considering both the en-face and the cross-sectional images, CNV was identified in 13 eyes with the rest OCT-A and in 22 eyes with the stress OCT-A ($P = 0.001$). Cross-sectional imaging was more sensitive than en-face imaging in detecting neovascular blood flow signals under both rest ($P = 0.125$) and stress ($P = 0.001$) conditions. The quantitative analysis showed a significantly greater neovascular area and fractal dimension on the stress OCT-A ($P = 0.002$).

• CONCLUSIONS: Performing OCT-A during HGT enhances the sensitivity of the examination in detecting CNV in chronic CSCR. The increased neovascular perfusion following the induced increase of blood pressure is consistent with choroidal blood flow dysregulation in patients with CSCR and indicates new areas of discussion about CNV in this disease. (Am J Ophthalmol 2020;211:63–75. © 2019 The Author(s). Published by Elsevier Inc. This is an open access article under the CC BY-NC-ND license (http://creativecommons.org/licenses/by-nc-nd/4.0/).)

THE PATHOPHYSIOLOGICAL MECHANISMS UNDERLYING the clinical manifestations of central serous chorioretinopathy (CSCR) are still not entirely clear. Cumulating observations, mostly obtained with indocyanine green angiography and optical coherence tomography (OCT), indicate the choroid is the primary seat of damage in this disease.[1–3] A pachychoroid, detectable with enhanced depth imaging OCT, is a common finding in patients with CSCR; thus, it is included in a spectrum of disorders that share this feature.[4]

Retinal pigment epithelium (RPE) dysfunction and abnormalities are other peculiar findings that contribute to the characterization of different phenotypic aspects, as well as acute or chronic stages of CSCR.[4–6] Variably shaped pigment epithelium detachments (PEDs) is a usual finding during the progression of the disease.[6] Serous dome-shaped PEDs are classic lesions that virtually always exist in acute CSCR. Flat, irregular PEDs (FIPEDs), described more recently, are frequently observed in patients with chronic CSCR.[6–8] Particular attention has lately been focused on FIPEDs because of their possible association with type 1 choroidal neovascularization (CNV).[9,10] Neovascular complications in chronic CSCR are apparently rare, based on the findings of studies using conventional multimodal imaging (e.g., fluorescein and indocyanine green angiography, OCT, and fundus autofluorescence).[9,10] Recent studies using OCT-angiography (OCT-A), a label-free imaging modality that relies on blood cell motion as the contrast,[11] suggest that CNV may frequently be associated with FIPEDs in CSCR.[12,13]

Accepted for publication Oct 24, 2019.

From the Fondazione per la Macula Onlus, Dipartimento di Neuroscienze (M.L., C.M.E., M.N., S.T., F.C.P.), Riabilitazione, Oftalmologia, Genetica e Scienze Materno-Infantili (DINOGMI), University Eye Clinic, Genova, Italy; Department of Biomedical and Surgical Sciences, Section of Ophthalmology (M.L.,C.C.), University of Perugia, S. Maria della Misericordia Hospital, Perugia, Italy; Centre Ophtalmologique de l'Odéon (M.L.), Paris, France; Department of Internal Medicine (D.F.), University of Perugia, S. Maria della Misericordia Hospital, Perugia, Italy; Department of Surgical Sciences, Eye Clinic (C.M.E.), University of Torino, Torino, Italy; Clinica Oculistica DINOGMi (M.N.), Università di Genova, Ospedale Policlinico San Martino, Genova, Italy; and the Instituto de Oftalmologia Dr. Gama Pinto (D.C.), Lisboa, Portugal

Inquiries to: Dr. Felice Cardillo Piccolino, Fondazione per la Macula Onlus, Dipartimento di Neuroscienze, Riabilitazione, Oftalmologia, Genetica e Scienze Materno-Infantili (DINOGMI), University Eye Clinic, Viale Benedetto XV 5, 16132, Genova, Italy; e-mail: felice.cardillopiccolino@gmail.com

The authors recently conducted OCT-A during rest and during an isometric stress to evaluate the response of choroidal and retinal blood flow to an abrupt elevation of blood pressure (BP) and ocular perfusion pressure (OPP).[14,15] Under this experimental condition, OCT-A showed increased perfusion of the choriocapillaris and retinal vessels in patients with CSCR. This finding demonstrated a defect in the physiological compensatory mechanisms that regulate blood flow in these vascular districts.

The aim of the present study was to evaluate whether OCT-A conducted during a stress test (stress OCT-A) would improve the visualization of CNVs in FIPEDs of patients with chronic CSCR compared to OCT-A conducted in the resting condition (rest OCT-A). The results of the study could provide new insights to discuss pathophysiological and clinical aspects concerning this particular type 1 CNV occurring in chronic CSCR.

SUBJECTS AND METHODS

• **DESIGN:** This prospective cohort study was conducted at the Fondazione per la Macula Onlus (Genova, Italy) and the Eye Clinic at S. Maria Della Misericordia Hospital (Perugia, Italy). Consecutive patients with chronic CSCR and macular FIPEDs were examined with OCT-A during rest and during an isometric exercise with the hand-grip test (HGT). Informed written consent was obtained from all enrolled patients. The study was conducted in accordance with the Declaration of Helsinki. The Genova and Perugia Institutional Ethics Committees granted study approval.

• **POPULATION:** Patients with a documented history of chronic CSCR and FIPEDs in the central macula were consecutively enrolled between February 2018 and July 2018. The initial diagnosis of CSCR was based on the presence of idiopathic serous macular detachment associated with choroidal thickening (detected with OCT-A), and RPE focal leakage and choroidal vascular hyperpermeability (detected with fluorescein angiography and indocyanine green angiography, respectively). Chronic CSCR was defined as the presence of symptoms for more than 6 months.[16] Eyes were selected that had macular FIPEDs with or without actual serous retinal detachment on structural OCT cross-sectional scans. An FIPED was an irregular elevation of the RPE under which the Bruch's membrane (BM) was visible on structural OCT B-scans.[13] The study eye was randomly selected in patients with bilateral disease and bilateral FIPEDs. To maintain a consistent phenotype, patients who had a pachychoroid but no history of serous retinal detachment, or those who had polypoidal choroidal vasculopathy revealed by dye angiography were excluded. Other ocular exclusion criteria were refractive errors >3 diopters, previous ocular surgery, or laser photocoagulation, photodynamic therapy (PDT) in the previous 12 months, or any evidence of an eye disease that might have interfered with the purpose of the study. Systemic exclusion criteria were hypertension (systolic BP >150 mm Hg or diastolic BP >90 mm Hg) for safety reasons, and diabetes, due to its frequent association with a condition of microvascular hemodynamic dysregulation that could have affected the results of the study.[17] Poor quality OCT-As that had a quality index lower than 30 were also excluded. All enrolled participants underwent a complete ophthalmological evaluation, which included best corrected visual acuity (BCVA) testing, baseline intraocular pressure measurement, fundus evaluation, structural OCT, and OCT-A (at baseline and during an isometric exercise). Previous intake of corticosteroids or PDT were also recorded.

• **IMAGING ACQUISITION PROTOCOL:** A spectral domain OCT device, the Spectralis OCT2 (Heidelberg Engineering, Heidelberg, Germany), was used to obtain the OCT-A. High-resolution OCT-A volume scans were acquired on a $10^{\circ} \times 10^{\circ}$ (3 mm × 3 mm) surface centered on the fovea. Each OCT-A volume scan consisted of 512 B-scans with 6 μm distance between consecutive B-scans (7 frames were averaged in each B-scan).

An OCT-A software viewer (Heyex version 1.9.201.0 software; Heidelberg Engineering, Heidelberg, Germany) was used to assess C-scans (i.e., "en-face") and cross-sectional angiograms. For the purpose of this study, the en-face and cross-sectional images were evaluated. The Heyex software uses an automated segmentation algorithm for the outer retinal layers. The inner and outer boundaries for this segmented slab were the outer plexiform layer-outer nuclear layer interface and BM respectively. For segmentation errors in the automatically segmented images, en-face angiograms were obtained immediately above the BM with a 40-μm thick section in which the boundaries were aligned on the BM's profile. Choroidal neovascularization was indicated by a hyperintense decorrelation signal inside the FIPED, which was visible on the en-face or cross-sectional OCT-A scans.[13]

Each patient underwent 2 OCT-A scanning sessions at baseline and during the HGT using the Jamar hand dynamometer (Lafayette Instruments, Lafayette, Indiana). Stress OCT-A began 1.5 minutes after beginning the exercise, when an increase in BP and OPP occur.[14,15] BP was simultaneously measured with an electronic sphygmomanometer (Omron model M6; Omron Europe BV, Hoofddorp, the Netherlands). Further details on the experimental protocol of the study have been previously reported.[14]

The same experienced operator (M.L.) conducted the 2 OCT-A imaging sessions within a single visit. Two investigators (F.C.P. and M.L.) independently reviewed all scans to ensure correct segmentation and image quality for the post hoc assessment.

• **QUALITATIVE IMAGING ANALYSIS:** Two experienced examiners (F.C.P. and M.L.) separately evaluated the en-face images and cross-sectional images. Each patient's rest and stress OCT-A were compared to detect possible changes in CNV imaging. Neovascular lesions visible on the en-face OCT-A were morphologically evaluated, based on previously described criteria.[11,18] In the cross-sectional images, at least 20 consecutive B-scans in the FIPED area were analyzed to determine the presence or absence of any hyperintense flow signal due to CNV between BM and the RPE. The presence (score 1) or absence (score 0) of a hyperintense flow signal in each OCT-angiogram were graded in a binary fashion. Potential shadow graphic artifacts that may have negatively influenced the vascular flow detection between BM and the RPE were taken into consideration.

The qualitative assessment of CNVs on en-face OCT-A scans included a subtraction protocol that highlighted the focal stress-induced changes of vascular perfusion. An image calculator tool (FIJI [an expanded version of ImageJ software], version 1.51h; National Institutes of Health, Bethesda, Maryland) was used to obtain differential images from the two contrast-enhanced OCT-A with one image obtained during the HGT and the other image obtained at baseline.

• **QUANTITATIVE IMAGING ANALYSIS:** A neovascular CSCR subgroup of patients with CNV on en-face OCT-A in the rest condition was selected for quantitative assessments of variations in vascular perfusion during the HGT. Quantitative OCT-A image analysis was conducted using a previously validated custom graphical user interface built in MATLAB coding language (version r2018a; MathWorks, Inc., Natick, Massachusetts).[19] Images were binarized using the Phansalkar thresholding algorithm (Dolby Laboratories, Inc., San Francisco, California), using a 15-pixel radius, which is a specific algorithm for low-contrast images.[20] Speckle noise filtering was obtained by using a median filter with a two-pixel radius. Small non-connected pixels (i.e., <10 contiguous pixels) were removed. The density map was computed, and the final CNV shape was determined. Quantitative OCT-A analyses of the blood flow area, vessel perfusion density (VPD), fractal dimension (FD), and lacunarity index (LAC) were issued using a graphical interface. The VPD was the percentage of the CNV area occupied by vessels. The box counting method at multiple origins was applied to the image of the binary skeleton to estimate the FD and LAC of the vascular network, which are global indices of morphological complexity and structural non-uniformity, respectively.[21,22] Box sizes followed the power of 2 series until a box of half-image pixel size was achieved. The results were then automatically exported into a different file for statistical analyses. Quantitative OCT-A variables were then correlated with the hemodynamic data of the same selected sample.

• **STATISTICAL ANALYSIS:** Quantitative variables are presented as the mean and standard deviation. The absolute and relative differences (i.e., ratio of the absolute difference to the baseline value) between the baseline data and under-stress quantitative data were also reported. The Shapiro-Wilk test was used to determine whether the sample was a normally distributed population. Depending on the statistical distribution, the mean values of the independent variables were compared using the Student *t* test or the Mann-Whitney *U* test. The paired *t* test or Wilcoxon-Mann-Whitney test was used to compare paired data. The Pearson *r* or Spearman rank correlation coefficient was used to measure the statistical dependence of quantitative variables. The McNemar test was used to compare cross-sectional and en-face qualitative variables. A *P* value of <0.05 was statistically significant. All statistical analyses were conducted using SAS release version 9.4 software (SAS Institute, Cary, North Carolina) for Windows (Microsoft, Redmond, Washington).

RESULTS

• **STUDY POPULATION:** In the study period, the screened population consisted of 37 patients with chronic CSCR. Twenty-nine of these patients (which included 5 women [17.2%]) were enrolled in the study. They had a FIPED in the macular region and did not fit the previously specified exclusion criteria. The mean age of patients with CSCR was 46.4 ± 6.2 years old (range, 29-64 years). The ethnicity of the whole sample was white. The mean BCVA was 0.10 LogMAR (range, 0.5-0), and the mean intraocular pressure value was 13.4 ± 1.9 mm Hg. Sixteen patients (55%) had a history of PDT. At the time of examination, a variable amount of subretinal fluid was detected on structural OCT in 22 patients (75.9%). No adverse events were reported during simultaneous OCT-A acquisition and the HGT.

• **HEMODYNAMIC DATA:** Hemodynamic data of the entire sample are expressed as the mean and standard deviations (Table 1). The under-stress values were significantly increased from the baseline values ($P < 0.05$). During the HGT, systolic and diastolic BP reached definite hypertensive values in all patients. When separately assessing patients with and without CNV (detected in any OCT-A image), no statistically significant hemodynamic differences existed between the two groups in the baseline and HGT assessed parameters (Table 2).

• **QUALITATIVE IMAGING ANALYSIS:** The 2 readers had 100% agreement in their qualitative analyses of the OCT-A. No significant segmentation errors were reported in the CNV C-scan sections. In the entire sample, OCT-A (independent of the cross-sectional or en-face

TABLE 1. Hemodynamic Findings in Chronic CSCR Patients at Baseline and during the Isometric Handgrip Exercise and Their Absolute and Relative Differences

	Baseline		Under-Stress			Absolute Difference		Relative Difference		Ratio	
	Mean	SD	Mean	SD	*P* Value Paired Data[a]	Mean	SD	Mean	SD	Mean	SD
Intraocular pressure (mm Hg)	13.4	1.9									
Systolic blood pressure	124.9	10.6	161.6	15.0	0.0001	36.66	13.85	29.9%	12.0%	1.3	0.1
Diastolic blood pressure	81.6	8.1	103.5	11.4	0.0001	21.86	9.30	27.3%	12.1%	1.3	0.1
Heart rate	70.3	8.4	92.4	10.2	0.0001	22.14	7.65	32.4%	13.2%	1.3	0.1
Mean arterial pressure	96.0	8.3	122.8	11.7	0.0001	26.79	10.32	28.4%	11.5%	1.3	0.1
Ocular perfusion pressure	50.6	6.0	68.5	7.5	0.0001	17.86	6.88	36.4%	15.5%	1.4	0.2

CSCR = central serous chorioretinopathy.
[a]Wilcoxon test for repeated measures.

TABLE 2. Hemodynamic Findings in Chronic CSCR Patients with and without Choroidal Neovascularization at Baseline and during the Isometric Handgrip Exercise

	No CNV (n = 7)		CNV (n = 22)		
	Mean	SD	Mean	SD	*P* Values
Baseline					
IOP (mm Hg)	13.3	1.8	13.5	2.0	0.86
SBP	121.3	10.7	126.0	10.6	0.45
DBP	81.9	9.9	81.5	7.7	0.68
HR	71.0	8.6	70.0	8.6	0.66
MAP	95.0	9.4	96.4	8.1	0.80
OPP	50.0	6.7	50.8	5.9	0.92
Under-stress (HGT)					
SBP	156.9	8.4	163.0	16.4	0.32
DBP	104.7	10.5	103.1	11.9	0.66
HR	93.1	10.3	92.2	10.4	0.74
MAP	122.1	9.0	123.1	12.7	0.88
OPP	68.1	5.8	68.6	8.0	0.80

CNV = choroidal neovascularization; CSCR = central serous chorioretinopathy; DBP = diastolic blood pressure; HGT = hand-grip test; HR = hearth rate; IOP = intra-ocular pressure; MAP = mean arterial pressure; OPP = ocular perfusion pressure; SBP = systolic blood pressure.

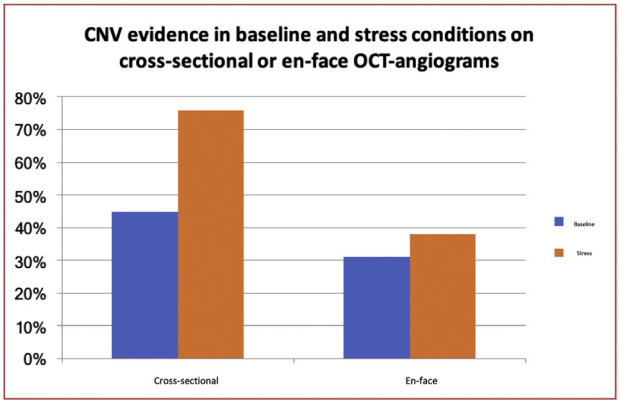

FIGURE 1. Improvement in CNV visualization between baseline and HGT OCT-A examination. The histograms show how the OCT-A examination, which was conducted under stress conditions (i.e., HGT), increased the capability of CNV detection. This approach is especially useful when using the cross-sectional approach for which the improvement is statistically significant (44.8% vs. 75.9%, respectively; $P = 0.001$). CNV = choroidal neovascularization; OCT = optical coherence tomography.

visualization) revealed CNV in 13 patients at baseline and in 22 patients during the HGT ($P = 0.001$). The analysis of the cross-sectional OCT-A showed a definite hyperintense flow signal between BM and the RPE in 13 patients (44.8%) at the baseline examination and in 22 patients (75.9%) during the HGT ($P = 0.001$) (Figure 1). On the en-face OCT-A, a well-delineated CNV network was visualized in 9 patients (31%) at baseline and in 11 patients (37.9%) during the HGT ($P > 0.05$) (Figure 1). Choroidal neovascularization was visualized in a higher number of patients on cross-sectional OCT-A than on en-face angiograms under the baseline condition (13 vs. 9 patients, respectively; $P = 0.125$) and during the stress test (22 vs. 11 patients, respectively; $P = 0.001$); the difference was statistically significant (Figure 2 and 3). In all cases where neovascular signals were detected on the rest OCT-A, they were also visible on the stress OCT-A.

For nine patients with CSCR for whom the baseline en-face OCT-angiogram revealed CNV inside the FIPED, stress OCT-A improved the visualization of the outline of the neovascular network and revealed vascular tracts and meshes, which were not visible initially. Differential OCT-A provided enhanced evidence of this finding (Figure 4).

In these lesions, tiny branching vessels, loops, peripheral anastomotic arcades, and a choriocapillaris hypointense

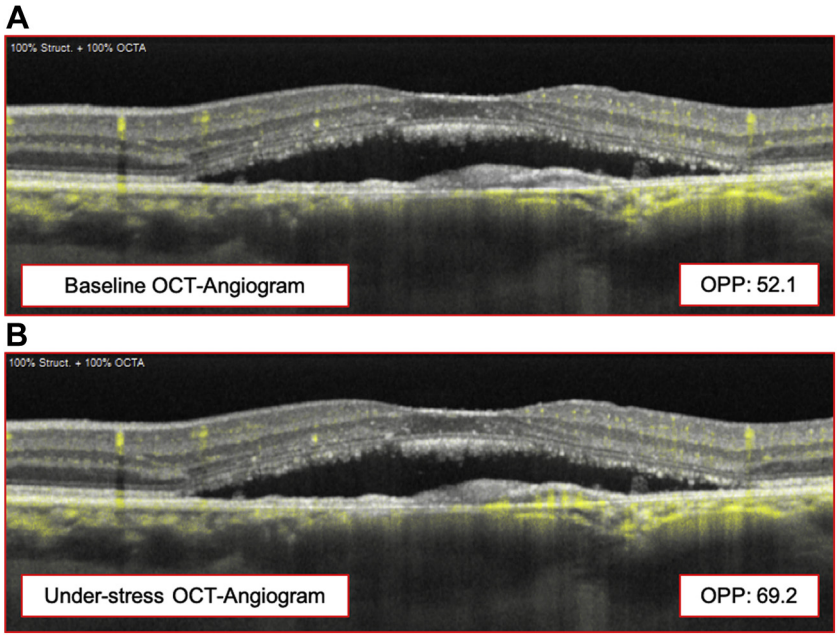

FIGURE 2. Cross-sectional OCT-angiography in a NV-CSCR case. Findings of CNV are seen in the resting condition and during HGT. (A, B) Obtained by averaging 5 consecutive B-scans in order to ensure the alignment of baseline and HGT OCT-A on a reference structural OCT (background). (A) No clear evidence of the flow signal (yellow) is seen within the FIPED during the baseline examination with an OPP of 52.1 mm Hg. (B) During the HGT, multiple flow signals resulting from a neovascular network are between Bruch's membrane and the detached RPE with an OPP of 69.2 mm Hg. FIPED = flat irregular pigment epithelial detachment; HGT = hand-grip test; NV-CSCR = neovascular central serous chorioretinopathy; OCT-A = optical coherence tomography-angiography; OPP = ocular perfusion pressure.

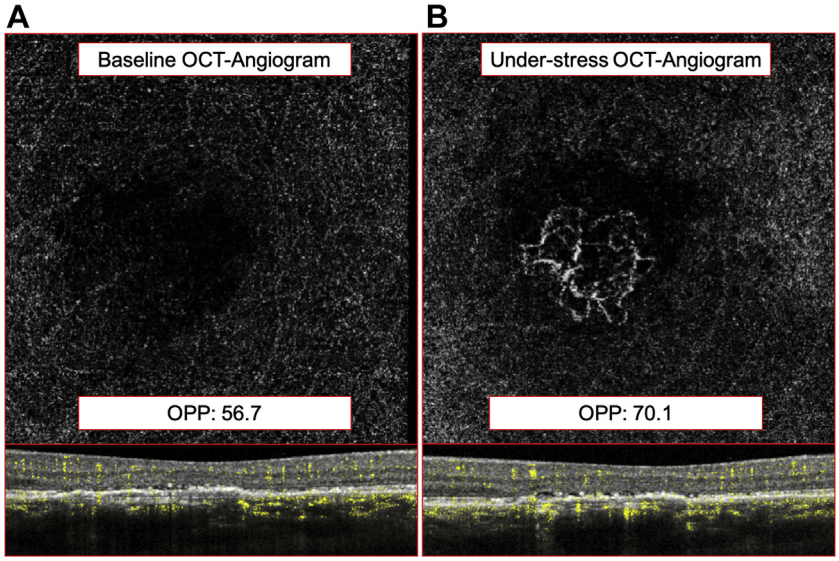

FIGURE 3. En-face OCT-angiography in a neovascular-CSCR case. CNV is seen in the resting condition and during HGT. (A) The baseline examination shows no evidence of CNV; the OPP is 56.7 mm Hg. (B) A neovascular network is clearly visible during the HGT; the OPP is 70.1 mm Hg. CNV = choroidal neovascularization; CSCR = central serous chorioretinopathy; HGT = hand-grip test; OCT = optical coherence tomography; OPP = ocular perfusion pressure.

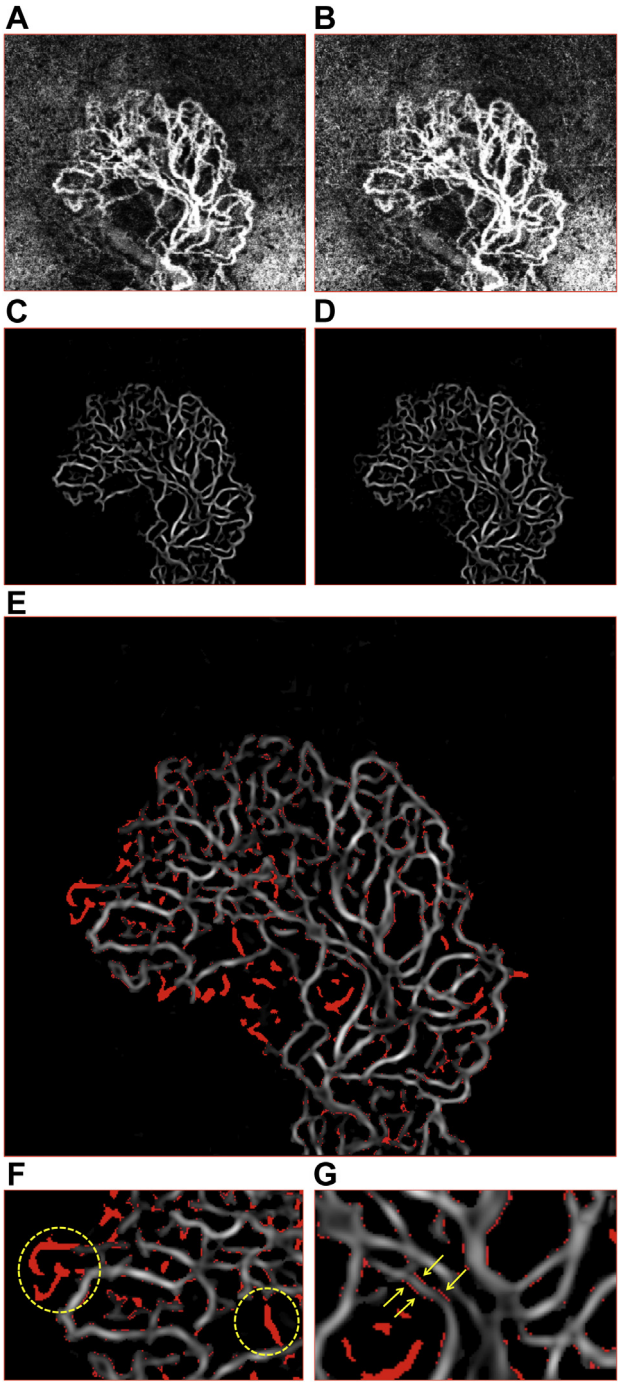

FIGURE 4. En-face OCT-angiography in a CSCR case. Type I choroidal neovascularization in the resting condition (A) and during the handgrip test (B). The contrast-enhanced images of the CNV at baseline (C) and during the HGT (D) after "vesselness" filtering, an in-built plugin of the FIJI software that helps to improve the visualization of the vascular structures and to suppress non-vascular structures and image noise. (E) The differential OCT-angiogram. The CNV at baseline is indicated by the gray neovascular network, whereas the red tracts represent an increase in blood flow during the HGT. (F, G) Increased blood flow allows the visualization of vascular tracts ([F] yellow dashed lines) and decorrelation signals at the borders of the vessel ([G] yellow arrows) that were hidden in resting conditions. CNV = choroidal neovascularization; CSCR = central serous chorioretinopathy; HGT = hand-grip test; OCT-A = optical coherence tomography.

halo, which are all biomarkers of choroidal neovascular activity in age-related macular degeneration (AMD),[11,18] involved fewer than one-third of the lesions or were undetected.

The qualitative assessment of cross-sectional OCT-A scans in neovascular cases frequently revealed focal flow signals straddling the BM. They were not shadow graphic artifacts produced by retinal vessels or CNVs, as exactly generated at the level or in proximity of the BM. These "crossing-signs," appeared as a connection of the neovascular lesion (i.e., the feeding or draining vessel) with the choroid (Figure 5, 6, and 7).

Among 22 patients in whom the complete OCT-A examination revealed CNV, 18 (82%) had a variable amount of subretinal fluid. This group included 18 of 22 eyes (82%) in which CNV was visible on cross-sectional OCT-A and 9 of 11 eyes (82%) in which CNV was detected on en-face angiograms. In eyes without any evidence of CNV in the rest and stress OCT-As, fluid was detected in 4 of 7 patients (57%). The association of subretinal fluid with detectable CNV on OCT-A was statistically nonsignificant ($P = 0.4$). It was also nonsignificant for patients with a neovascular network visible on the en-face angiograms ($P = 0.9$).

To evaluate the potential impact of CNV on visual acuity, we compared the BCVA of eyes in whom stress/rest en-face OCT-A revealed a well-delineated neovascular network (en-face score, 1), compared to the BCVA of eyes in which CNV was visualized only in the cross-sectional view or was not visible (en-face score, 0). The BCVA was 0.14 ± 0.16 LogMAR in the group with en-face = 1, and was 0.12 ± 0.16 LogMAR in the group with en-face = 0. The two groups were not significantly different ($P = 0.8$).

• **QUANTITATIVE IMAGING ANALYSIS:** The semi-automated quantitative assessment results of CNVs on en-face OCT-A are shown in Table 3. The blood flow area and FD of the CNV were significantly increased in the under-stress OCT-A compared to the baseline angiograms ($P = 0.002$). By contrast, the LAC index values were significantly decreased in the under-stress examination ($P = 0.002$) (Figure 8). A significant positive linear correlation existed between the baseline mean arterial pressure and OPP and the baseline VPD and under-stress VPD (Figure 9). No other significant correlations were observed between the hemodynamic findings and OCT-A quantitative parameters. Moreover, no significant correlations existed between corticosteroid therapies or previous PDT and hemodynamic or OCT-A quantitative data.

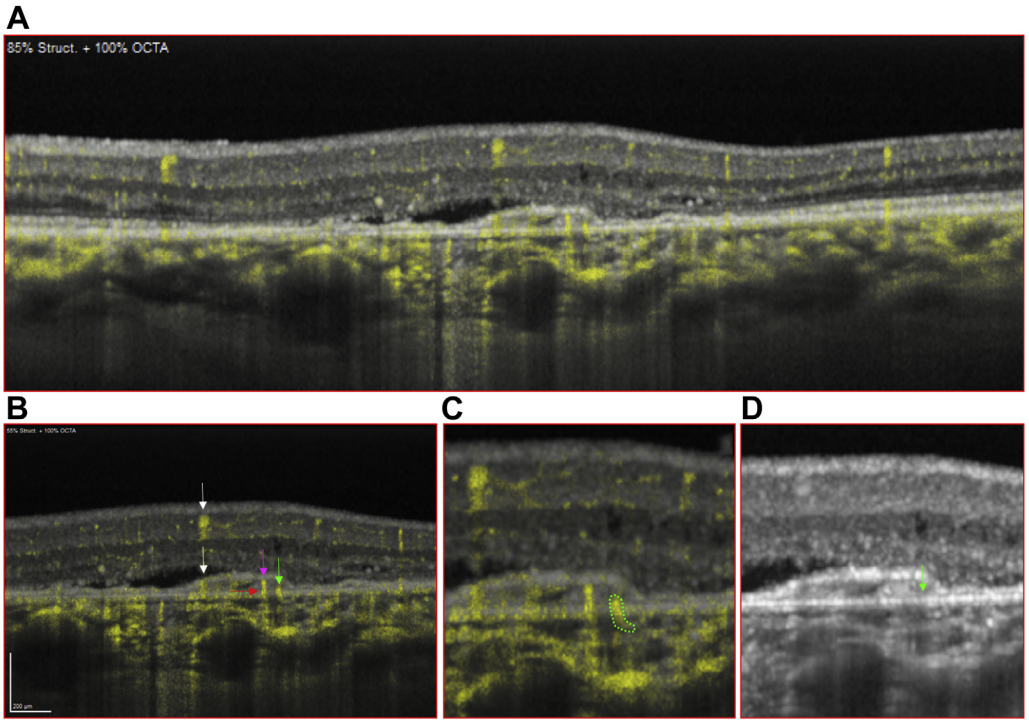

FIGURE 5. Cross-sectional OCT-angiogram taken during HGT showing flow signal crossing Bruch's membrane in a neovascular CSCR case. (A) The cross-sectional OCT-A image shows multiple flow-signals (yellow) within the FIPED. (B) Detail of the FIPED highlights the presence of a definite flow-signal due to CNV (pink arrow) and its shadow graphic artifact (red arrow), a shadow-graphic artifact of a retinal vessel (white arrows), and a wedge-shaped flow signal (green arrow) crossing Bruch's membrane. The latter was defined as the "crossing-sign." (C) This flow signal seems to continue in the choroid (greed dotted line) and appears as a feeder or draining vessel connecting the CNV with the choroid. This sign is typically visible in areas of reduced Bruch's membrane reflectivity ([D] green arrow). CNV = choroidal neovascularization; CSCR = central serous chorioretinopathy; FIPED = flat irregular pigment epithelial detachment; HGT = hand-grip test; OCT = optical coherence tomography.

DISCUSSION

THE AIM OF THE PRESENT STUDY WAS TO EVALUATE whether OCT-A conducted during a stress test would improve the visualization of CNV in FIPEDs of patients with chronic CSCR, compared to OCT-A conducted in the resting condition. In the present study, stress OCT-A conducted during isometric physical exercise with HGT was more sensitive than rest OCT-A in detecting CNV in FIPEDs associated with chronic CSCR.

Reports[4,12,13,23,24] have indicated that type 1 CNV within FIPEDs may be associated with chronic CSCR and more generally with a pachychoroid condition. OCT-A seems to have a greater capability than dye-enhanced angiography to reveal these neovascular structures.[13] Nevertheless, in published studies using OCT-A, the rate of CNV detection within FIPEDs has high variability, probably because of different patient selection criteria (i.e., inhomogeneous CSCR cohorts) or the different OCT-A imaging settings.[12,13,23,24] Bousquet and associates[13] and Bonini and associates[24] enrolled a phenotype of patients with CSCR that was substantially comparable to the patients in the present series. Those 2 studies analyzed en-face OCT-A and reported CNV detection in 35.6% (21 of 59) of eyes and in 30% of (8 of 27) eyes, respectively.[13,24] The present study obtained similar results by using the same type of evaluation (i.e., en-face rest OCT-A) and detected a defined neovascular structure in 31% of eyes (9 of 29). However, when conducting OCT-A during HGT, the rate of detecting CNV on en-face scans was 37% because a well-delineated CNV was detected in 2 additional patients who did not have a frank neovascular network at the baseline examination.

We extended the definition of vascularized FIPEDs to include patients in whom a neovascular network was not appreciable on the en-face OCT-A, although a clear flow signal existed between the BM and the RPE on cross-sectional images. With the latter type of evaluation, evidence of CNV affected 44.8% of patients in rest OCT-A, and significantly increased to 75.9% in the under-stress examination. Our results ultimately demonstrated that OCT-A has a higher sensitivity in revealing CNV in eyes with CSCR when using the HGT protocol and that cross-sectional analysis of angiograms may help identify false-negative case. Flat irregular pigment epithelial detachments are very frequent in cases of long-standing CSCR;

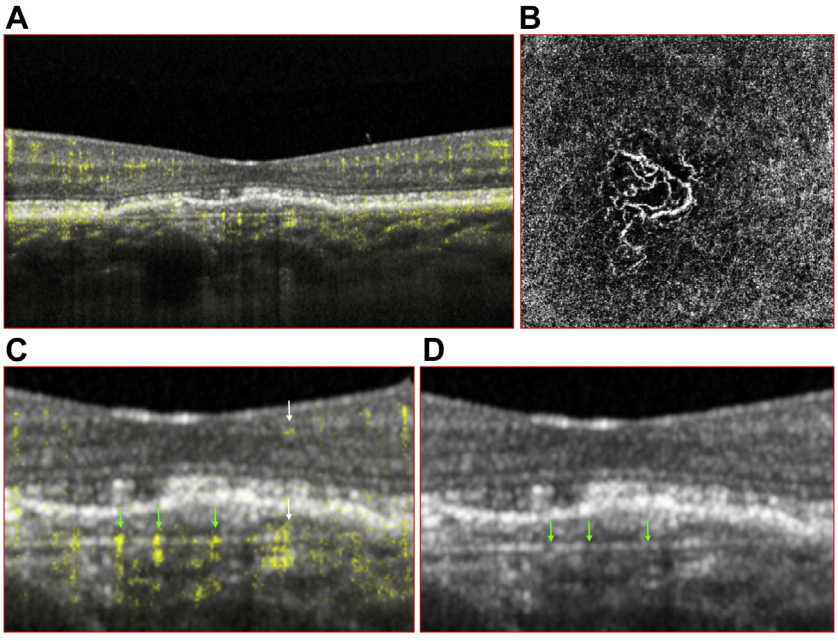

FIGURE 6. OCT-A during HGT in a neovascular CSCR case. (A) The cross-sectional OCT-A image shows multiple flow signals (yellow) crossing Bruch's membrane in the FIPED area. (B) En-face OCT-angiogram shows the entire neovascular network. (C) Detail of the FIPED highlights the presence of definite flow signals (green arrows) crossing Bruch's membrane and a shadowgraphic artifact of a retinal vessel (white arrows). These flow signals (defined as "crossing signs") are located in corresponding areas of reduced Bruch's membrane reflectivity on structural OCT ([D] green arrows). CSCR = central serous chorioretinopathy; FIPED = flat irregular pigment epithelial detachment; HGT = hand-grip test; OCT-A = optical coherence tomography-angiography.

therefore, the present findings indicated that most of these cases could be de facto complicated by CNV. Prospective studies could clarify whether the flow signals observed only in cross-sectional images represent an early stage of neovascularization that will progress toward a more structured lesion that is identifiable in the en-face mode.

On cross-sectional OCT-A, CNV seems to be characterized by focal decorrelation signals crossing the BM, which indicates a feeder vessel or draining flow to and from the choroid. This "crossing sign" could aid in identifying earlier stages of CNV. Their identification may be favored by a high axial resolution of the OCT-A device such as that the authors used (3.9 μm), which allows distinguishing different vascular details within a short axial distance.

Qualitative evaluation of CNV on the en-face OCT-A did not reveal definite identification of morphological patterns which suggest status of neovascular activity, based on previously reported parameters.[11,18] However, characterizing the morphological details of these lesions is beyond the scope of the present study.

On the en-face OCT-A, we also quantitatively evaluated the neovascular perfusion changes occurring during the hypertensive episode induced by the HGT. The analysis included the blood flow area and the VPD, which indicates neovascular extension, and the FD and LAC, which are measurements of the morphological vascular complexity. This assessment confirmed a significant increase in neovascular perfusion during the physical exercise. The FD and LAC parameters are widely used to describe vascular systems and their changes over time in angiogenesis.[25,26] An increase in the FD and a reduction in the LAC with stress OCT-A suggested increased blood flow within the thinner portion of the microvascular network where blood cell velocity may be too slow to be detected with rest OCT-A.

On analyzing the FD in active and quiescent CNVs in AMD, Al-Sheikh and associates[25] observed a higher vascular pattern complexity in active lesions (FD = 1.57) than in quiescent lesions (FD = 1.44). In the current study, the mean FD of the CNV was 1.46 at baseline, which was somewhat close to the value Al-Sheikh and associates[25] attributed to quiescent CNVs in AMD. For neovascular lesions complicating chronic CSCR, based on the preexisting basal exudative pattern proper of the disease, the definition of activity may not be simply founded on the evidence of subretinal or intraretinal exudation. Therefore, morphological biomarkers of neovascular activity could be particularly helpful. The aforementioned morphological analysis and the values of FD suggest that CNV complicating chronic CSCR may be classified as inactive.

Furthermore, a correlation between a detectable flow signal within the FIPEDs and the presence of subretinal

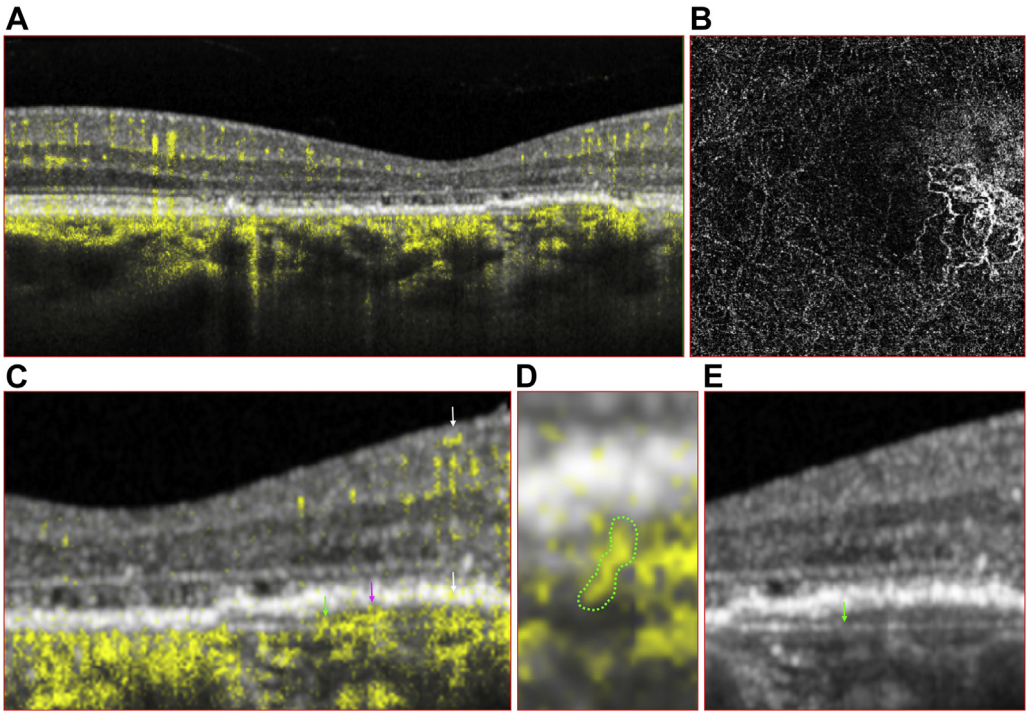

FIGURE 7. OCT-A during HGT in a neovascular CSCR case. (A) The cross-sectional OCT-A image shows multiple flow signals (yellow) within the parafoveal FIPED. (B) En-face OCT-angiogram shows a definite choroidal neovascular network. (C) Details of the FIPED highlight the presence of a flow signal due to CNV (pink arrow) between the RPE and Bruch's membrane. The shadow graphic artifacts of retinal vessels (white arrows) and a wedge-shaped flow signal (the "crossing-sign" [green arrow]) straddling Bruch's membrane are also visible. (D) Magnified visualization of the "crossing-sign" (green dotted line). The area of reduced Bruch's membrane reflectivity colocalizes the "crossing-sign" on structural OCT ([E] green arrow). CNV = choroidal neovascularization; CSCR = central serous chorioretinopathy; FIPED = flat irregular pigment epithelial detachment; HGT = hand-grip test; OCT = optical coherence tomography; RPE = retinal pigment epithelium.

TABLE 3. Quantitative OCT-Angiography Assessment of CNV in CSCR Patients at Baseline and during the Isometric HGT

	Baseline		Under Stress			Absolute Difference		Relative Difference		Ratio	
	Mean	SD	Mean	SD	*P* Value Paired Data[b]	Mean	SD	Mean	SD	Mean	SD
FD[a]	1.46	0.07	1.51	0.09	0.002	0.05	0.05	3.6%	3.4%	1.0	0.0
LAC-I [a]	3.36	1.59	2.77	1.06	0.002	−0.59	0.69	−14.6%	12.7%	0.9	0.1
Area [a]	8.09	10.41	9.15	10.63	0.002	1.06	0.79	31.5%	38.0%	1.3	0.4
VPD	0.67	0.20	0.68	0.16	0.625	0.02	0.11	4.8%	15.5%	1.0	0.2

CNV = choroidal neovascularization; CSCR = central serous chorioretinopathy; FD = fractal dimension; HGT = hand-grip test; LAC-I = lacunarity index; OCT = optical coherence tomography; VPD = vascular perfusion density.

[a]Statistically significant differences ($P < 0.05$).

[b]Wilcoxon test for repeated measures.

fluid was not observed. No correlation existed for CNVs that were only detectable in cross-sectional angiograms or for those well delineated on en-face angiograms. These observations suggested that the type of CNV we considered in the present study may be irrelevant for the exudative activity of CSCR. In addition, we did not observe in our patients a significant correlation between the presence of a well-delineated CNV and worse visual acuity. The clinical impact of CNVs within FIPEDs on the disease, and consequently the appropriateness of possible anti-vascular endothelium growth factor (anti-VEGF) treatment may therefore be questionable. On the other hand, it cannot be excluded that the successful role of PDT in chronic CSCR may be at least partly due to its effect on

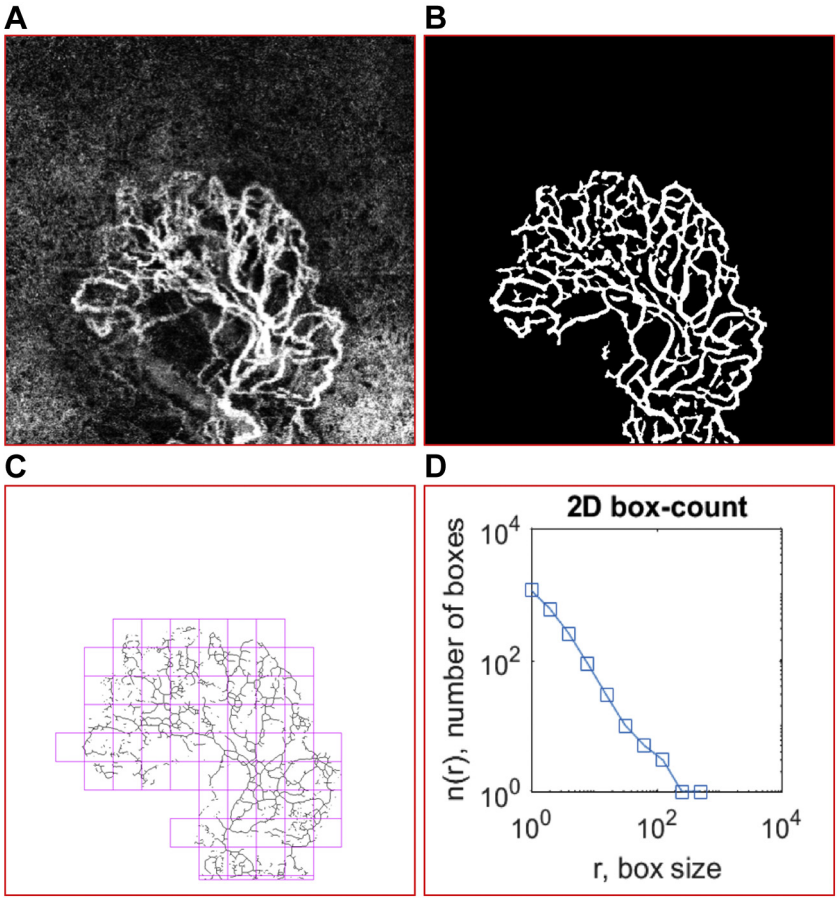

FIGURE 8. OCT -angiography images show the filtering schema of CNV complicating chronic CSCR. (A) En-face OCT-angiogram of the CNV, obtained by segmenting the volume scan between the RPE and Bruch's membrane. (B) Speckle noise removal and binarization of the image. (C) Box-counting approach on the skeletonized CNV. (D) Graphic output of the box-counting method, where "n" (i.e., the number of boxes needed to cover the set) as a function of "r" (i.e., the size of the boxes). The set is a fractal; therefore, a power-law relationship exists: [n = n0 r $^{(-DF)}$] in which "DF" is the fractal dimension. CNV = choroidal neovascularization; CSCR = central serous chorioretinopathy; OCT-A = optical coherence tomography; RPE = retinal pigment epithelium.

unsuspected areas of CNV.[27] Because of the limited number of examined patients, further investigations are needed to elaborate the possible exudative contribution of CNV in chronic CSCR. Analyzing changes in neovascular morphology and FD in the stress OCT-A could perhaps provide further indication of activity or quiescence by evidencing the portion of the presumedly less mature component of CNV where blood flow is slower.

In this study, poorly defined or nonvisible neovascular tracts at the baseline OCT-A examination became more appreciable when the blood pressure increased during the HGT. However, this differential behavior in the neovascular blood flow in the rest and stress conditions should not occur if the intrinsic mechanisms were efficient in regulating choroidal blood flow and protecting the choriocapillaris from abrupt elevations in the OPP.[28,29] Riva and associates[28] observed that the OPP in healthy young people can increase up to 67% before having repercussions on the choroidal blood flow. During the stress test, the increase in the OPP in the present patients was well below this value (36.4% ± 15.5%), although it had a relevant impact on the blood flow of the terminal microvascular network within the FIPEDs. These findings are consistent with an insufficient reactive increase in vascular resistance in the underlying choroidal vasculature. They practically support the concept of impaired choroidal blood flow regulation in CSCR, which has long been demonstrated with laser doppler flowmetry[30] and more recently with stress/rest OCT-A examination.[14,15]

In patients with dry AMD, Pournaras and associates[31] and Metelitsina and associates[32] used laser doppler flowmetry and did not observe significant choroidal blood flow changes during increased blood pressure after participants performed a squatting exercise. They concluded that these patients had no regulatory abnormality within the choroid.[31,32] However, Pournaras and associates[31] noted

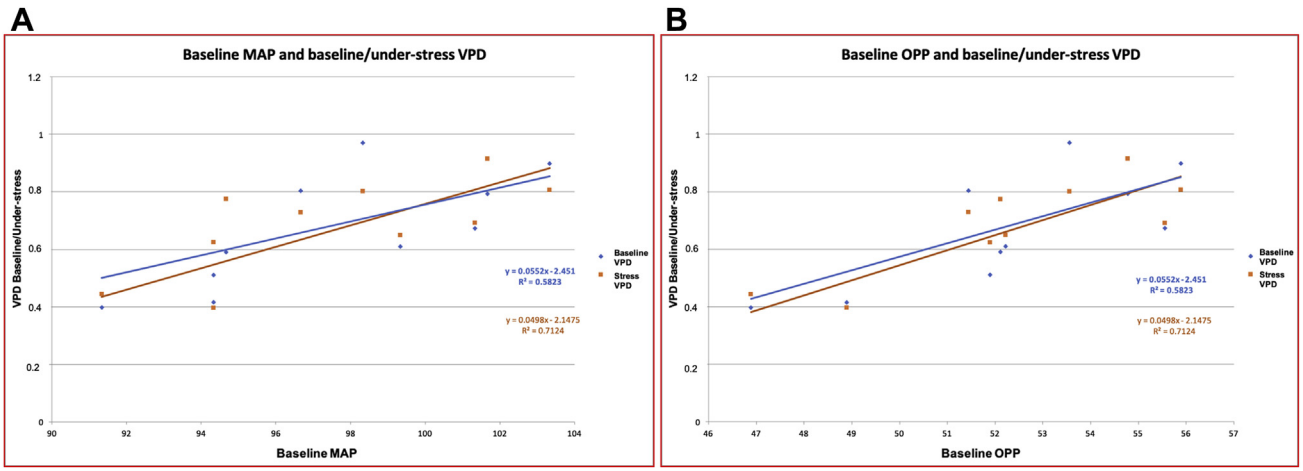

FIGURE 9. (A, B) Correlation between VPD and the MAP or ocular perfusion pressure (OPP). A positive linear correlation between the baseline MAP/OPP and VPD is shown for the baseline or during the HGT. These correlations indicate that higher values of MAP/OPP are associated with higher levels of CNV perfusion density. CNV = choroidal neovascularization; HGT = hand-grip test; MAP = mean arterial pressure; OPP = ocular perfusion pressure; VPD = vascular perfusion density.

increased subfoveal blood flow after the same stress test in patients with neovascular AMD. The authors attributed this finding to choroidal dysregulation characterizing neovascular AMD and to possible altered blood flow regulation within the neovascular tissue.[31] From these observations, the loss of the adaptation of choroidal vascular resistance to hemodynamic stress may be a discriminating factor between neovascular and non-neovascular AMD.[31] In chronic CSCR, choroidal dysregulation may be the basal pathology of the disease, and a causal link between this abnormality and the occurrence of CNV may be even more conceivable.

A wide amount of studies suggest the concept that mechanical cellular stress is an important regulator of protein synthesis and in the activation of several factors such as VEGF.[33,34] Experimental studies[35,36] have demonstrated that mechanical stretch induces the RPE to secrete VEGF, similar to other VEGF-expressing cells such as cardiac myocytes and mesangial cells.[33,34] Seko and associates[34] demonstrated that short periods of stretching (1-3 hours), but not prolonged stretching, induce in vitro RPE cells to produce VEGF. Kinoshita and associates[36] observed that cyclic stretch and hypertension increased intracellular succinate in RPE cells and the expression of VEGF.

Patients with CSCR are often hypertensive and easily reach high levels of blood pressure during physical effort, as shown in the present study and in previous reports.[14,15] They are characterized by sympathetic hyperactivity favoring emotional stress, increased blood pressure, and hemodynamic instability.[37] Intrinsic compensation mechanisms in the choroid are lacking; therefore, the choriocapillaris in these patients is likely affected by recurrent hemodynamic stresses that also mechanically impact the RPE. The condition of stretching the RPE cells in the CSCR is already clinically testified by RPE detachments, which are detected by OCT in virtually all patients with this disease. These authors hypothesize that the neovascular process that develops in the chronic form of CSCR within FIPEDs may result from stretch-induced VEGF expression by the RPE. This pathogenic peculiarity could explain the lower activity of these neovascular lesions than that of other CNVs in which a more relevant amount of VEGF is primarily produced by inflammation and hypoxia. Based on the high rate of CNV associated with FIPEDs in our patients, we speculate that, in the early stage, the hyperreflective content of FIPEDs, which presumedly include large plasma proteins with proangiogenic activity, may represent a newly formed extracellular matrix that is a prelude to neovascularization.[38] The possible link between CNV and hemodynamic factors in patients with chronic CSCR is also suggested by the positive linear correlation between the baseline mean arterial pressure and OPP and the VPD of the neovascular lesions.

A limitation of the present study is the small sample size, even though it was phenotypically well characterized. Moreover, the qualitative evaluation of OCT-A could be negatively affected because of its intrinsic subjective nature. The limits of the technology used for imaging neovascular blood flow must be considered. A smaller inter-B scan distance (<6 μm) may allow for detection of additional flow signals within the FIPEDs that were missed with the available scanning protocols. Finally, continuous monitoring of the hemodynamic parameters, rather than serial detection, could provide a better analysis of systemic changes induced by HGT, and consequently a better correlation with changes on OCT-A.

In conclusion, this study demonstrated that OCT-A performed during HGT improved visualization of CNV

developing within FIPEDs in chronic CSCR, which may limit false negative results. Our findings indicated that FIPEDs in the CSCR were vascularized in most patients. Thus, the authors hypothesize that their appearance may predict a progression to neovascularization. However, the clinical impact of this type 1 CNV in CSCR remains unclear and deserves further investigation.

The increased perfusion of CNVs that was observed during the experimental increase in BP was consistent with dysregulation of choroidal blood flow, for which systemic hemodynamic stresses were not diminished before reaching terminal choroidal microcirculation. By using an isometric exercise, we experimentally reproduced hypertensive episodes that may occur frequently in everyday life and, in patients with CSCR, may produce recurrent overperfusion of the choriocapillaris and mechanical stress on the RPE. Experimental studies[34–36] have demonstrated that hypertension and cyclic stretch induce RPE cells to produce VEGF; therefore, we speculate that insufficient choroidal vascular reactivity and the associated exposure of the RPE to hemodynamic stresses may be involved in CNV development in CSCR.

A stress/rest protocol, using physical and pharmacological stress, is exploited in myocardial perfusion imaging and echocardiography to obtain functional and anatomical information on blood flow through the coronary arteries and the heart muscle.[39] The application of the stress modality in OCT-A, which was used in the present study and in previous studies,[14,15] obtained findings of clinical and pathologic interest on chorioretinal microcirculation and neovascularization in CSCR. The same stress/rest OCT-A protocol, which is easily executable using the HGT, may increase the potential of OCT-A in the study of chorioretinal microcirculation in other conditions, such as diabetes, where physical exercise may be able to early highlight hemodynamic dysfunctions.[40]

ALL AUTHORS HAVE COMPLETED AND SUBMITTED THE ICMJE FORM FOR DISCLOSURE OF POTENTIAL CONFLICTS OF INTEREST and none were reported.

FUNDING/SUPPORT: This work was supported by Fondazione per la Macula Onlus, Genova, Italy, and Fondazione Piera, Pietro and Giovanni Ferrero, Alba, Italy.

FINANCIAL DISCLOSURES: M.L. is a consultant for Bayer (Whippany, New Jersey), Novartis (Morristown, New Jersey), Allergan (Bridgewater Twp., New Jersey), and Heidelberg Engineering (Heidelberg, Germany). All other authors reported no financial support or financial conflict of interest.

REFERENCES

1. Cardillo Piccolino F, Borgia L, Zinicola E, Zingirian M. Indocyanine green angiographic findings in central serous chorioretinopathy. *Eye* 1995;9:324–332.
2. Imamura Y, Fujiwara T, Margolis RO, Spaide RF. Enhanced depth imaging optical coherence tomography of the choroid in central serous chorioretinopathy. *Retina* 2009;29:1469–1473.
3. Yang L, Jonas JB, Wei W. Choroidal vessel diameter in central serous chorioretinopathy. *Acta Ophthalmol* 2013;91:358–362.
4. Cheung CM, Lee WK, Koizumi H, Dansingani K, Lai TY, Freund KB. Pachychoroid disease. *Eye (Lond)* 2019;33:14–33.
5. Lee WJ, Lee JH, Lee BR. Fundus autofluorescence imaging patterns in central serous chorioretinopathy according to chronicity. *Eye (Lond)* 2016;30:1336–1342.
6. Song IS, Shin YU, Lee BR. Time-periods characteristics in the morphology of idiopathic central serous chorioretinopathy evaluated by volume scan using spectral-domain optical coherence tomography. *Am J Ophthalmol* 2012;154:366–375.
7. Mitarai K, Gomi F, Tano Y. Three-dimensional optical coherence tomographic findings in central serous chorioretinopathy. *Graefes Arch Clin Exp Ophthalmol* 2006;244:1415–1420.
8. Fujimoto H, Gomi F, Wakabayashi T, Sawa M, Tsujikawa M, Tano Y. Morphologic changes in acute central serous chorioretinopathy evaluated by Fourier-domain optical coherence tomography. *Ophthalmology* 2008;115:1494–1500.
9. Fung AT, Yannuzzi LA, Freund KB. Type 1 (sub-retinal pigment epithelial) neovascularization in central serous chorioretinopathy masquerading as neovascular age-related macular degeneration. *Retina* 2012;32:1829–1837.
10. Hage R, Mrejen S, Krivosic V, Quentel G, Tadayoni R, Gaudric A. Flat irregular retinal pigment epithelium detachments in chronic central serous chorioretinopathy and choroidal neovascularization. *Am J Ophthalmol* 2015;159:890–903.
11. Coscas GJ, Lupidi M, Coscas F, Cagini C, Souied EH. Optical coherence tomography angiography versus traditional multimodal imaging in assessing the activity of exudative age-related macular degeneration: a new diagnostic challenge. *Retina* 2015;35:2219–2228.
12. Quaranta El Maftouhi M, El Maftouhi A, Eandi CM. Chronic central serous chorioretinopathy imaged by optical coherence tomographic angiography. *Am J Ophthalmol* 2015;160:581–587.
13. Bousquet E, Bonnin S, Mrejen S, Krivosic V, Tadayoni R, Gaudric A. Optical coherence tomography angiography of flat irregular pigment epithelium detachment in chronic central serous chorioretinopathy. *Retina* 2018;38:629–638.
14. Cardillo Piccolino F, Lupidi M, Cagini C, et al. Choroidal vascular reactivity in central serous chorioretinopathy. *Invest Ophthalmol Vis Sci* 2018;59:3897–3905.
15. Cardillo Piccolino F, Lupidi M, Cagini C, et al. Retinal vascular reactivity in central serous chorioretinopathy. *Invest Ophthalmol Vis Sci* 2018;59:4425–4433.
16. Daruich A, Matet A, Dirani A, et al. Central serous chorioretinopathy: recent findings and new physiopathology hypothesis. *Prog Retin Eye Res* 2015;48:82–118.

17. Stehouwer DDA. Microvascular dysfunction and hyperglycemia: a vicious cycle with widespread consequences. *Diabetes* 2018;67:1729–1741.
18. Coscas F, Lupidi M, Boulet JF, et al. Optical coherence tomography angiography in exudative age-related macular degeneration: a predictive model for treatment decisions. *Br J Ophthalmol* 2019;103:1342–1346.
19. Coscas F, Cabral D, Pereira T, et al. Quantitative optical coherence tomography angiography biomarkers for neovascular age-related macular degeneration in remission. *PLoS One* 2018;13:e0205513.
20. Phansalkar N, More S, Sabale A, et al. Paper ID 154: adaptive local thresholding for detection of nuclei in diversely stained cytology images. 2011 International Conference on Communications and Signal Processing; 2011;218–220.
21. Masters BR. Fractal analysis of the vascular tree in the human retina. *Annu Rev Biomed Eng* 2004;6:427–452.
22. Tolle CR, McJunkin TR, Gorsich DJ. An efficient implementation of the gliding box lacunarity algorithm. *Physica D* 2008; 237:306–315.
23. Dansingani KK, Balaratnasingam C, Klufas MA, Sarraf D, Freund KB. Optical coherence tomography angiography of shallow irregular pigment epithelial detachments in pachychoroid spectrum disease. *Am J Ophthalmol* 2015;160: 1243–1254.
24. Bonini Filho MA, de Carlo TE, Ferrara D, et al. Association of choroidal neovascularization and central serous chorioretinopathy with optical coherence tomography angiography. *JAMA Ophthalmol* 2015;133:899–906.
25. Al-Sheikh M, Iafe NA, Phasukkijwatana N, Sadda SR, Sarraf D. Biomarkers of neovascular activity in age-related macular degeneration using optical coherence tomography angiography. *Retina* 2018;38:220–230.
26. Landini G, Murray PI, Misson GP. Local connected fractal dimensions and lacunarity analyses of 60 degrees fluorescein angiograms. *Invest Ophthalmol Vis Sci* 1995;36:2749–2755.
27. Cardillo Piccolino F, Eandi CM, Ventre L, Rigault de la Longrais RC, Grignolo FM. Photodynamic therapy for chronic central serous chorioretinopathy. *Retina* 2004;23:752–763.
28. Riva CE, Titze P, Hero M, Movaffaghy A, Petrig BL. Choroidal blood flow during isometric exercises. *Invest Ophthalmol Vis Sci* 1997;38:2338–2343.
29. Lovasik JV, Kergoat H, Riva CE, Petrig BL, Geiser M. Choroidal blood flow during exercise-induced changes in the ocular perfusion pressure. *Invest Ophthalmol Vis Sci* 2003;44:2126–2132.
30. Tittl M, Maar N, Polska E, Weigert G, Stur M, Schmetterer L. Choroidal hemodynamic changes during isometric exercise in patients with inactive central serous chorioretinopathy. *Invest Ophthalmol Vis Sci* 2005;46: 4717–4721.
31. Pournaras CJ, Logean E, Riva CE, et al. Regulation of subfoveal choroidal blood flow in age-related macular degeneration. *Invest Ophthalmol Vis Sci* 2006;47:1581–1586.
32. Metelitsina TI, Grunwald JE, DuPont JC, Ying G. Effect of isometric exercise on choroidal blood flow in patients with age-related macular degeneration. *Br J Ophthalmol* 2010;94: 1629–1631.
33. Li J, Hampton T, Morgan JP, Simons M. Stretch-induced VEGF expression in the heart. *J Clin Invest* 1997;100:18–24.
34. Seko Y, Seko Y, Takahashi N, Shibuya M, Yazaki Y. Pulsatile stretch stimulates vascular endothelial growth factor (VEGF) secretion by cultured rat cardiac myocytes. *Biochem Biophys Res Commun* 1999;254:462–465.
35. Seko Y, Seko Y, Fujikura H, Pang J, Tokoro T, Shimokawa H. Induction of vascular endothelial growth factor after application of mechanical stress to retinal pigment epithelium of the rat in vitro. *Invest Ophthalmol Vis Sci* 1999;40:3287–3291.
36. Kinoshita H, Suzuma K, Maki T, et al. Cyclic stretch and hypertension increase retinal succinate: potential mechanisms for exacerbation of ocular neovascularization by mechanical stress. *Invest Ophthalmol Vis Sci* 2014;55:4320–4326.
37. Lucini D, Norbiato G, Clerici M, Pagani M. Hemodynamic and autonomic adjustments to real life stress conditions in humans. *Hypertension* 2002;39:184–188.
38. Neve A, Cantatore FP, Maruotti N, Corrado A, Ribatti D. Extracellular matrix modulates angiogenesis in physiological and pathological conditions. *Biomed Res Int* 2014;2014: 756078.
39. O'Keefe JH Jr, Barnhart CS, Bateman TM. Comparison of stress echocardiography and stress myocardial perfusion scintigraphy for diagnosing coronary artery disease and assessing it severity. *Am J Cardiol* 1995;75:25D–34D.
40. Roberto S, Crisafulli A. Consequences of type 1 and type 2 diabetes mellitus on the cardiovascular regulation during exercise: a brief review. *Curr Diabetes Rev* 2017;13: 560–565.